Macromolecules

Article

Effect of Comonomer Sequence Distribution on the Adsorption of Random Copolymers onto Impenetrable Flat Surfaces

Young K. Jhon, James J. Semler, Jan Genzer, Martin Beevers, Olga A. Gus'kova, Pavel G. Khalatur, and Alexei R. Khokhlov

Macromolecules, **2009**, 42 (7), 2843-2853• DOI: 10.1021/ma8027936 • Publication Date (Web): 09 March 2009

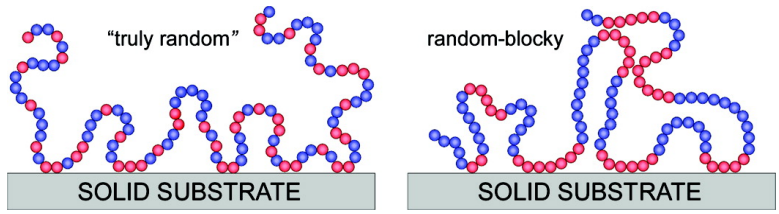

More About This Article

Additional resources and features associated with this article are available within the HTML version:

- Supporting Information
- Access to high resolution figures
- Links to articles and content related to this article
- Copyright permission to reproduce figures and/or text from this article

View the Full Text HTML

Macromolecules is published by the American Chemical Society. 1155 Sixteenth Street N.W., Washington, DC 20036

Effect of Comonomer Sequence Distribution on the Adsorption of Random Copolymers onto Impenetrable Flat Surfaces

Young K. Jhon,[†] James J. Semler,[†,#] Jan Genzer,*[,†] Martin Beevers,[‡] Olga A. Gus'kova,[§] Pavel G. Khalatur,*[,§,∥] and Alexei R. Khokhlov[∥,⊥]

Department of Chemical & Biomolecular Engineering, North Carolina State University, Raleigh, North Carolina 27695-7905, Department of Chemical Engineering & Applied Chemistry, Aston University, Birmingham B4 7ET, United Kingdom, Institute of Organoelement Compounds, Russian Academy of Sciences, Moscow 119991, Russia, Department of Polymer Science, University of Ulm, Ulm D-89069, Germany, and Physics Department, Moscow State University, Moscow 119899, Russia

Received December 15, 2008; Revised Manuscript Received January 27, 2009

ABSTRACT: We study the effect of comonomer sequence distributions in random copolymers (RCPs) on RCP adsorption on flat impenetrable surfaces. RCP poly(styrene-*co*-4-bromostyrene) (PBr_xS), where x denotes the mole fraction of 4-bromostryrene (4-BrS), is prepared by bromination of parent homopolystyrene. By varying the solvent quality during the bromination, either "truly random" (good solvent) or "random-blocky" (poor solvent) PBr_xS RCPs are prepared. Adsorption studies of PBr_xS from various solvents at silica surfaces reveal that the adsorption of PBr_xS increases with (1) increasing blockiness of the macromolecule, (2) increasing content of 4-BrS in PBr_xS, and (3) decreasing solvent quality. Additionally, the effect of comonomer sequence distribution on RCP adsorption is modeled in detail using a coarse-grained statistical mechanical model and fully atomistic simulations based on configurational-biased grand-canonical Monte Carlo (CB-GCMC) technique. The main result from the simulations can be summarized as follows: (1) Increasing the degree of "blockiness" in comonomer distribution enhances the adsorption of macromolecules dissolved in a good solvent. (2) Near the adsorption transition, the amount of adsorbed segments in "random-blocky" copolymers is larger relative to their regular multiblock counterparts. (3) Lowering the solvent quality facilitates copolymer adsorption. Overall, the findings from computer modeling are found to be in a good agreement with the experimental data.

Introduction

Adsorption of organic macromolecules to inorganic substrates (e.g., glass, silica, mica, and metals) significantly affects the performance of a large body of various applications and interfacial phenomena, including (but not limited to) chromatographic columns, polymer coatings, adhesion media, paints, stabilization of colloidal particles, flocculation, cell adhesion, and biocompatibility of artificial organs in medicine.[1−7] Adsorption of polymers to surfaces is very different from that of small molecules. Whereas attaching a segment of a polymer coil to the surface increases the probability of adsorption for adjacent segments of the same molecule, the adsorption probability for small molecules remains equal for all molecules. The well-known loop−train−tail model describes the conformations of isolated polymer chains as a function of the adsorption energy.[8−17] From an enthalpic standpoint, polymers always tend to maximize the number of contacts between the adsorbing units along the chain and the adsorbing sites on the surface. This limits the total number of possible conformations that polymer chains can adopt as well as their translational mobility, resulting in an overall entropy loss. At equilibrium, a balance between the enthalpy gain and entropy loss due to adsorption is established, which, in turn, determines the equilibrium conformations of adsorbing polymers.

Over the past few decades, many theoretical, experimental, and computer simulation studies have been carried out that aimed at investigating the conformation of end-functionalized homopolymers or block copolymers near interfaces. The principal factors that govern the behavior of such heteropolymers as they approach a flat, impenetrable surface include: (1) the strength of the interaction between the adsorbing segments along the chain and the adsorbing sites on the surface and the polymer's ability to replace any adsorbed molecular displacers (e.g., solvent molecules adsorbed to the surface), (2) chemical and molecular polydispersity of the polymer, (3) polymer solubility in a given solvent, and (4) sequence distribution of the monomers comprising the polymer chain. As confirmed by many researchers, the sequence distribution of the adsorbing segments greatly affects the adsorption characteristics of such heteromacromolecules.[18−31] A large body of work has been devoted to understanding the adsorption of diblock copolymers (A-*b*-B), in which segments (e.g., A) of one of the blocks (adsorbing/anchor) possess a greater affinity toward the surface than segments (e.g., B) of the other block (buoy). Whereas the A units tend to maximize the number of favorable contacts with the surface, thereby increasing the enthalpy gain, the B segments help to alleviate the entropy losses by allowing the buoy block to dangle in the solution. Having their A and B segments distributed evenly throughout the entire length of the chain, alternating copolymers (A-*alt*-B) represent the other extreme of the monomer sequence distribution spectra. Provided that the B segments do not experience too strong of a repulsion from the surface, the adsorption properties of A-*alt*-B will be similar to homopolymers that possess some effective average of A and B homopolymer adsorption properties. Forming loop, tail, and train conformations depends on the balance of maximizing the number of A segments in contact with the surface and the number of B segments extended into the bulk. This causes the chain to occupy a large amount of surface area when adsorbed to the surface while maintaining long enough loops and tails, which help to alleviate any translational and conformational entropy losses.

* Corresponding authors. E-mail: Jan_Genzer@ncsu.edu (J.G.); khalatur@polly.phys.msu.ru (P.G.K.).
[†] North Carolina State University.
[‡] Aston University.
[§] Russian Academy of Sciences.
[∥] University of Ulm.
[⊥] Moscow State University.
[#] Present address: Lexmark International, Lexington, KY.

10.1021/ma8027936 CCC: $40.75
Published on Web 03/09/2009

Random copolymers (RCPs, A-*co*-B) represent a special case of macromolecules; their adsorption properties, which fall somewhere between those of diblock and alternating copolymers,[32] are expected to depend on the distribution of the A and B comonomers. Note that unlike the case of A-*b*-B or A-*alt*-B copolymers the monomer sequence distributions in A-*co*-B RCPs are disordered.[33−35] Motivated by the connection of RCPs to biopolymers, such as proteins and nucleic acids,[36] computer simulations and various theoretical approaches have been employed that provide insight into the principles of adsorption of RCPs.[37−41] Several studies have established the effects of solvency and coverage,[42] the effect of architecture of the polymer on the structure of the adsorbed layer,[43] and the thermodynamic properties of the RCPs.[44−46] If the monomer sequence in this chain is "truly random", then there will be both long and short runs of consecutive adsorbing segments within the same chain. Upon adsorption, the longer consecutive adsorbing blocks will be preferentially located at the adsorbing surface while contributing to an increase in the overall enthalpy gain due to adsorption. Concurrently, loops and tails will be formed that do not necessarily contain only long sequences of nonadsorbing blocks but also adsorbing segments; these conformations help alleviate any tendency to completely "zip" the macromolecule to the surface, which would be too costly entropically. Increasing the relative block size of the consecutive runs of adsorbing segments within the copolymer (we later refer to this as "blockiness") also increases the size of the consecutive runs of nonadsorbing segments, which are expected to constitute major portions of loops and tails. Having longer "blocks" of adsorbing and nonadsorbing segments is expected to promote stronger adsorption of such "random-blocky" RCPs (relative to truly random RCPs). The larger block lengths of adsorbing segments increase the probability of localizing such RCPs at surfaces; longer runs of nonadsorbing segments facilitate larger loops and longer tails, which decrease the entropic penalty associated with localizing the RCP at the surface.

Most experimental work dealing with adsorption of RCPs at surfaces primarily concentrated on investigating the effect of the copolymer composition and chain length.[15,37,38] Whereas some computer simulations appeared that studied the effect of monomer sequence distribution on adsorption of RBCs on surfaces,[29,47] we are not aware of any experimental study that would demonstrate the effect of comonomer sequences on the partitioning of RCPs at interfaces. The aim of this work is to provide insight into the effect that governs the adsorption of RCPs on flat impenetrable surfaces as a function of copolymer chemical composition, solvent quality, and comonomer sequence distribution on adsorption. We will demonstrate that increasing the degree of "blockiness" (i.e., the length of the consecutive adsorbing segments along the copolymer) enhances the adsorption of RCPs at flat, impenetrable surfaces.

The article is organized as follows. In the next section, we briefly describe the procedure leading to the formation of RCPs with tunable randomness and provide information about the adsorption experiments. The description of the computer simulation models used to provide molecular insight into the adsorption follows. We then discuss the results of the adsorption of homopolymers and RCPs from various solvents onto flat silica surfaces. A discussion of the experimental and simulations results is provided next.

Materials and Methods

Synthesis of Poly(styrene-*co*-4-bromostyrene). In this work we use poly(styrene-*co*-4-bromostyrene) (PBr_xS, where x denotes the mole fraction of the 4-bromostyrene (4-BrS) unit) RCPs. The polymers were prepared by bromination of parent polystyrenes (PSs) following the mechanism of an electrophilic substitution of bromine onto the phenyl ring of PS. To tune the monomer distribution of the 4-BrS units along the macromolecule, we perform the bromination reaction under different solvent conditions. As discussed by a series of molecular simulation studies[48−54] and experimentally verified by a few research groups,[55−57] the monomer distribution of the so-called "coloring species" (bromine, in our case) depends on the instantaneous size of individual homopolymer coils (PS, in our case). Specifically, bromination of PS performed under good solvent conditions leads to PBr_xS RCPs that have a random distribution of the 4-BrS units. In contrast, decreasing the solvent quality causes the parent PS coils to collapse, and bromination in such cases produces RCPs with random-blocky monomer sequences; that is, there are longer runs of consecutive 4-BrS units relative to the monomer distribution in truly random RCPs.[58] In our previous publications, we have performed a thorough analysis of the bromination process under various solvents conditions[59] and presented quantitative information about the average monomer distribution by measuring the molar Kerr constant,[58] which bears information about polymer stereoregularity, chemical composition, and comonomer sequence distribution. Because the polymer stereoregularity is known a priori (we used atactic PS homopolymers) and chemical composition is measured independently by elemental analysis and nuclear magnetic resonance, the Kerr effect measurements provide unambiguous information about the comonomer sequence in PBr_xS RCPs.[58,60,61] In our previous work, we have also shown that whereas bromination carried out at 33 °C in 1-chlorodecane (CD) (θ temperature, T_θ = 6.6 °C) led to PBr_xS RCPs with random distribution of 4-BrS (denoted as r-PBr_xS), the same polymer modification performed in 1-chlorododecane (CDD) (T_θ = 58.6 °C) produced random-blocky PBr_xS RCPs (denoted as b-PBr_xS).[58]

Monodisperse atactic PS (M_n = 30 kDa, polydispersity index = 1.06) was purchased from Pressure Chemical (Pittsburgh, PA). Tetrahydrofuran (THF), toluene (TOL), cyclohexane (CH), CD, CDD, nitrobenzene (NB), and bromine were purchased from Aldrich and used as received. r-PBr_xS and b-PBr_xS RCPs were prepared using the same protocol as that in ref 58. $PBr_{1.0}S$ was synthesized in NB. An appropriate amount of PS in a given solvent (CD or CDD) at 1% (w/w) concentration was below the overlap concentration, c^*, estimated to be about 4% (w/w).[62] The solution was then placed in a controlled temperature cell, and the cell was subjected to a temperature cycle. Specifically, the cell was ramped to 70 °C (well above T_θ of all solvents) and maintained for 60 min. Afterward, the cell temperature was lowered to 32.8 °C at a rate of 0.3 °C/min and maintained for 60 min. After the equilibration was completed, a three-fold stoichiometric excess of bromine was added to the solution under dark conditions. We have empirically established the time needed to produce PBr_xS with a given "degree of bromination", x. After a predetermined amount of time, the reaction was terminated by the addition of a few drops of 1-pentene. The samples were then dissolved in TOL and precipitated in methanol. This purification step was repeated at least three times to eliminate any residual bromine and remaining solvent (CD or CDD). The polymer was then dried at 60 °C under vacuum to remove all remaining traces of methanol. The concentration of bromine in the samples was determined by elemental analysis (Atlantic Microlabs, Norcross, GA) and ^{13}C NMR. More details of the characterization of PBr_xS copolymers are provided in refs 58 and 59. In our previous work, we established that the average block length of the consecutive 4-BrS units within b-$PBr_{0.60}S$ was ∼20. Kerr effect experiments from b-$PBr_{0.35}S$ were performed using the same protocol as that outlined in our previous publication.[58] Modeling the experimental data using the rotational isomeric state (RIS) model revealed that the average block length of the consecutive 4-BrS units within b-$PBr_{0.35}S$ was ∼3. We assume that the comonomer sequence distribution in b-$PBr_{0.26}S$ (also used in this work) is close to that of b-$PBr_{0.35}S$. No Kerr effect data are available for b-$PBr_{0.10}S$. However, on the basis of the values obtained from the b-$PBr_{0.35}S$ and b-$PBr_{0.60}S$ RCPs and on previous observations supported by incomplete data sets,[63] it is safe to

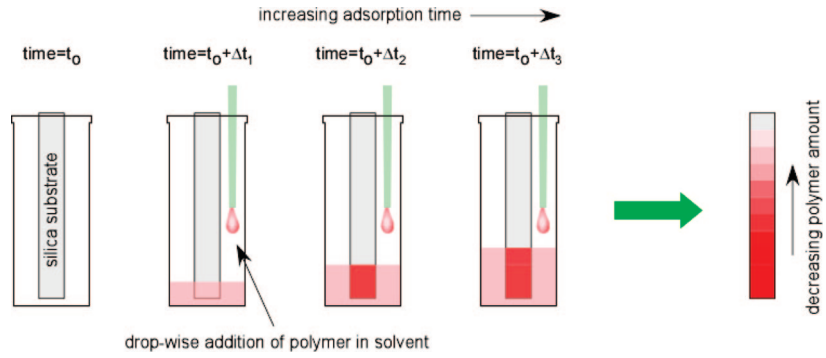

Figure 1. Schematic illustrating the combinatorial set up for polymer adsorption onto flat silica surfaces.

assume that the average block length of the consecutive 4-BrS units in b-$PBr_{0.10}S$ is <3.

Adsorption of Poly(styrene-*co*-4-bromostyrene) Random Copolymers onto Silica Surfaces. Our study of polymer adsorption onto surfaces was conducted using a combinatorial method illustrated pictorially in Figure 1. Specifically, a silicon wafer (orientation [100], supplied by Silicon Valley Microelectronics) was cut into 1 × 5 cm^2 pieces, washed with acetone, blow dried with nitrogen gas, and exposed for 15 min to ultraviolet/ozone (UVO) treatment. The latter procedure removed any organic impurity present on the surface of the wafer and generated surface-bound hydroxyl groups on silica. The wafer was then placed vertically into a custom-built adsorption apparatus consisting of a sample holder suspended in a 20 mL glass vial. Polymer solution (1 to 2% w/w) in either TOL, THF, or CH was added dropwise to the vial from the top via attached tubing. The polymer solution level increased with time, thereby producing a continuous gradient of adsorbed polymer layer on the surface; the bottom part of the sample had the thickest layer and the top part had the thinnest layer of PBr_xS. Upon completion of the adsorption experiments, the sample was removed from the adsorption apparatus, washed several times with the same solvent used for adsorption measurement, and blow dried with nitrogen gas. The amount of polymer present on the sample was quantified with ellipsometry as a function of the position on the wafer. The ellipsometric thickness was measured using a variable angle spectroscopy ellipsometer (J.A. Woollam) and evaluated using an index of refraction of PBr_xS, n_{PBr_xS}, that corresponded to the weighted average (linear effective medium approximation[64]) of the refractive indices of pure PS ($n = 1.591$) and $PBr_{1.0}S$ ($n = 1.62$) at 633 nm[65] weighted by the composition determined by the elemental analysis. We then determined the total polymer adsorbed amount by multiplying the film thickness by the density of PBr_xS ($\rho_{PBr_xS} = 1.051 + 0.0541x$).[66] In the above analysis, we assumed that n_{PBr_xS} and ρ_{PBr_xS} depended primarily on the content of 4-BrS and were independent of the comonomer distribution and in the sample.

Computer Simulation. Theoretical modeling offers useful insight into polymer adsorption onto surfaces that can complement experimental data and, in some cases, also provide fundamental information that is difficult or impossible to obtain experimentally. In the present study, two models have been employed. The first model (I) is a "minimal" statistical mechanical model for which the results obtained should be relatively general. Here we use a semianalytical−seminumerical approach developed in ref 67 to investigate the selective adsorption of regular and random multiblock copolymers onto a flat, chemically homogeneous surface. The second model (II) reflects the properties of a fully atomistic system.

Model I. The block copolymer was modeled as a Gaussian chain having $N-1$ steps ($N = 360$) on a simple cubic lattice. We considered two-letter (AB) copolymer chains with rigid bonds of fixed length b (= 1) and the chemical AB composition fixed at 1:1. The chain was placed in a self-closed slab (with periodic boundary conditions applied in the x and y directions) between two impenetrable planes located at $z = 0$ and $z = bN$. The $z = 0$ plane was chosen to be an adsorbing surface. For a given chain configuration, the system energy was defined as $E = -\varepsilon_A n_A - \varepsilon_B n_B - \varepsilon_S(n_{AS} + n_{BS})$, where n_A and n_B are the number of A-type and B-type monomers such that their z coordinate is $z = 0$ and n_{AS} and n_{BS} are the number of monomer−solvent contacts. The monomer unit A was chosen to exhibit strong attractive interaction of strength $\varepsilon_A \equiv \varepsilon = 1$ with the surface sites, whereas B monomers had weaker adsorption energy of strength $\varepsilon_B = \varepsilon/2$. To make a parallel to the experimental studies discussed, the A monomers correspond to the 4-BrS units of a partially brominated polystyrene (PBr_xS) adsorbing onto silica surfaces. In most of the calculations, for ε_S, we set $\varepsilon_S = \varepsilon/2$ so that the solvent was good both for A and B monomers. Because contacts with the substrate usually entail a reduction of monomer−solvent contacts, there are two competing forces that affect the formation of the adsorption layer. The energy parameter, ε, is measured in k_BT units with $k_B = 1$. In the model, the binding affinity of the copolymer to the surface is determined by the reduced temperature, $T = k_BT/\varepsilon$, as well as by the distribution of the A and B segments along the chain backbone.

In this work, we studied periodic (alternating) multiblock copolymers A-*alt*-B. They can be represented as $(A_LB_L)_m$, where L is the fixed block length and $m = N/2L$. To examine the effect of randomness in the distribution of monomers, we also performed calculations for AB copolymers in which the lengths of continuous A and B runs, l, in a sequence were determined by the Poisson distribution $f(l) = e^{-L}L^l/l!$, where L represents the average block length. This represents one of the simplest cases of RCPs with a monomodal block size distribution. For RCPs, the lengths of the segments composed of the units of a given type, L_A and L_B, are random quantities. One can regard such systems with a given polydispersity of block lengths to be a mixture of "polymer species", each labeled by the values of l_A and l_B. Those systems can thus be considered to be polydisperse generalizations of single-component systems $(A_LB_L)_m$ with fixed block lengths. Here and below, under the term "polydispersity", we mean the variance of the block size distribution. For the sake of simplifying our discussion, we restricted our analysis to the symmetric case: $L_A = L_B = L$ and $\varphi_A = \varphi_B = 1/2$, where $\varphi_\alpha = N_\alpha/N$, α = A, B, and $N_A + N_B = N$.

It has been established that the "coloring scheme" outlined in the experimental section produces copolymers with a specific monomer sequence distribution described by the statistics of the Lévy-flight (or "proteinlike") type.[68] For such probabilistic processes, an observable stochastic variable (block size, in our case) exhibits large jumps ("flights"), termed "Lévy flights",[69] which are characterized by a power-law (rather than exponential) probability distribution function. We additionally carried out calculations for RCPs with the Lévy-flight (LF) statistics. (For more detail, see ref. 68.) Here we again restricted the calculations to the aforementioned symmetric case. The probability distribution of block lengths, $\boldsymbol{l}$, in proteinlike copolymers can be written as[68]

$$f_A(l) = \frac{\pi b}{3R^*}\sum_{n=1}^{\infty} n(-1)^{n+1}\sin\left(\frac{n\pi b}{R^*}\right)\exp\left[-\frac{b^2}{6}\left(\frac{n\pi}{R^*}\right)^2 l\right] \quad (1)$$

for A units and

$$f_B(\ell) = \frac{1}{3(2^{1/3}-1)^2}\sum_{n=1}^{\infty}\frac{\zeta_n^2 \sin\left(\zeta_n \frac{b/R^* - 1}{2^{1/3}-1}\right)}{\zeta_n - \sin\zeta_n \cos\zeta_n} \times \exp\left[-\frac{b^2}{6}\left(\frac{\zeta_n}{R^*(2^{1/3}-1)}\right)^2 \ell\right] \quad (2)$$

for B units. Here $R^* = b(3N/8\pi)^{1/3}$ and ζ_n satisfies $\zeta_n = (1 - 2^{-1/3})\tan\zeta_n$. Note that this distribution is not a "true" LF distribution, which falls to 0 as $1/|x|^{\alpha+1}$ (where $0 < \alpha < 2$) and therefore has an infinite variance, but represents the so-called truncated Lévy flight (TLF) with a finite variance D for finite chain lengths.[69,68] As has been shown,[68] the copolymers generated with the use of eqs 1 and 2 reproduce the "coloring" procedure described in refs 48−50: Monomers located in the core of the globule are set to be A type, whereas monomers belonging to a globular surface are assigned to be of B type.

The algorithm for calculating the adsorption properties was based on recurrence procedures for evaluating the single-chain partition function of a copolymer chain.[67] In this article, we primarily address the dependence of energetic quantities on temperature and chain architecture in adsorption equilibrium.

Model II. For the fully atomistic model, computer simulations have been carried out in the grand-canonical ensemble, where the chemical potentials rather than the number of adsorbed poly(styrene-*co*-4-bromostyrene) macromolecules were fixed. The chief purpose of these simulation studies was to model a polymer solution that was in equilibrium with adsorbent at constant temperature and chemical potential of the macromolecules. Basic GCMC simulations of rigid molecules typically include four different move types: insertions, deletions, translations, and rotations.[70] For exploring the intramolecular degrees of freedom of flexible polymers, CB-GCMC based on the Rosenbluth sampling method was employed.[71,72] An insertion was done by attempting to grow a chain in an atom-by-atom fashion inside a self-closed slab. Starting from annealed amorphous silica surface with dangling oxygen atoms,[73] a super-lattice was created to obtain a periodic lattice of size 57.02 × 57.02 Å^2 in the x and y directions. To generate the hydroxylated silica surface, free oxygen atoms were saturated by hydrogen atoms on both faces, with the resulting distance between the oxygen atoms on the opposite sides of about 33.07 Å. An empty space, $\Delta z = 50$ Å, was added to the simulation cell in the z direction. The disordered surface is characterized by regions that are hydrophilic and hydrophobic, depending on the presence of silanol (Si-OH) groups. The positions of the substrate atoms were fixed because physisorption is not expected to alter the geometry of the substrate surface, whereas polymer atoms were allowed to move in the simulation procedure. The energies were computed using the well-parametrized polymer-consistent class II force field (PCFF).[74,75] The partial charges were assigned according to the PCFF force field. The atom-based summation method was used to evaluate the nonbonded van der Waals interactions with a cutoff distance of 15 Å. The standard Ewald method was used for evaluating Coulomb interactions. For generating adsorption isotherms, 20 000 000 steps were required before both energy and the loaded amount converged to their final values. Each simulation point obtained at a given temperature and pressure followed these steps.

It should be noted that because our model I is based on a simple Gaussian chain that does not include any parameter concerning chain−chain interactions, the aggregation of adsorbed chains is not possible. This model describes single-chain adsorption from a dilute solution and provides a general framework for calculating properties of the copolymers with a given monomer sequence distribution. Model II is a fully atomistic model for which multiple chain adsorption is possible.

Results and Discussion

Experimental Results. As a starting point in our discussion, let us examine the adsorption of PS and $PBr_{1.0}S$ homopolymers onto silica surfaces from various solvents. These results provide a benchmark for our discussion of the adsorption characteristics of PBr_xS RCPs. In Figure 2, we plot the amount of PS (□) and $PBr_{1.0}S$ (○) adsorbed from (a) THF, (b) TOL, (c) CH at 25 °C, and (d) CH at 50 °C onto flat silica surfaces as a function of adsorption time. Recall that the amount of adsorbed polymer depends on the interplay between polymer solubility in the solvent, the affinity of the polymer for the substrate, and the ability of the polymer segments to replace solvent molecules at the solid/liquid interface. Whereas the latter two parameters can, in principle, be lumped together, we keep them separated for the sake of simplifying our discussion.

In Table 1, we list the Flory−Huggins (F−H) interaction parameters, χ, for PS/solvent and $PBr_{1.0}S$/solvent couples. PS should be readily dissolved in all solvents because $\chi \leq 0.5$. Recall that $\chi = 0.5$ corresponds to the θ condition, which separates the good solvent ($\chi < 0.5$) and poor solvent ($\chi > 0.5$) states. As a result, the tendency of PS to separate from the solvent and adsorb onto the silica surface should be relatively small. Considering that in all cases, the PS chains have the same molecular weight, the differences in adsorbed PS amounts on SiO_x seen in Figure 2 can be attributed to different abilities of PS chains to replace the solvent molecules at the SiO_x/solution interface. Because THF is known to interact with SiO_x very strongly through polar interactions,[79] the replacement of THF by styrene segments at the solution/silica interface is rather difficult. TOL molecules are likely attached to the hydrated silica though relatively weak hydrogen bonds. (Note that there is always going to be a small number of water molecules present at the silica surface.)[80] Eventually, some of the TOL molecules get misplaced by styrene segments allowing PS to adsorb. Because CH interacts with silica primarily via van der Waals interactions,[81] its replacement with styrene segments is relatively easy because this process allows for the formation of more strong hydrogen bonds between styrene and hydrated silica. This is clearly documented by the rapid adsorption of PS onto silica (Figure 2c,d) at early adsorption times. The small but detectable difference in total adsorbed PS amount on silica reported in Figure 2c,d can be attributed to the slight difference in solubility of PS in CH at different temperatures. Recall that whereas at 25 °C CH acts as a θ solvent, at 50 °C CH becomes a good solvent for PS. The θ temperature of PS in CH is ∼34 to 35 °C.[82] In the latter case, PS chains prefer to stay solvated by CH more strongly relative to the case of the poor solvent conditions.

$PBr_{1.0}S$ is less soluble in THF and TOL than PS and is completely insoluble in CH. Moreover, the solubility of $PBr_{1.0}S$ in THF is higher than that in TOL. Whereas data for the solubility of $PBr_{1.0}S$ in THF are not available, we assume that $\chi_{4\text{-BrS/THF}} < \chi_{4\text{-BrS/TOL}}$; at large polymer concentration in TOL ($\phi_2 > 0.95$), $PBr_{1.0}S$ precipitates out, whereas it remains completely soluble in THF. The tendency of $PBr_{1.0}S$ to adsorb onto silica is relatively strong. By assuming that styrene segments interact with silica athermally (i.e., $\chi_{S/SiO_x} \approx 0$), Oslanec and coworkers reported the value of adsorption F−H parameter for $\chi_{4\text{-BrS/SiO}_x}$ to be ∼−0.07.[83] The latter value can thus be thought of as a difference in the adsorption energy between 4-BrS and styrene monomers on silica surface. Considering both decreased solubility of 4-BrS and stronger affinity toward SiO_x, the adsorbed amount of $PBr_{1.0}S$ chains on silica surfaces should exceed that of PS. This is clearly documented by the data in Figure 2a,b. Without knowing the actual values of the THF/SiO_x and TOL/SiO_x interactions, it is not easy to deconvolute the effect of the bulk solubility and the ability of 4-BrS to replace the solvent molecules at the silica interface. The only definite conclusion we can make is that the

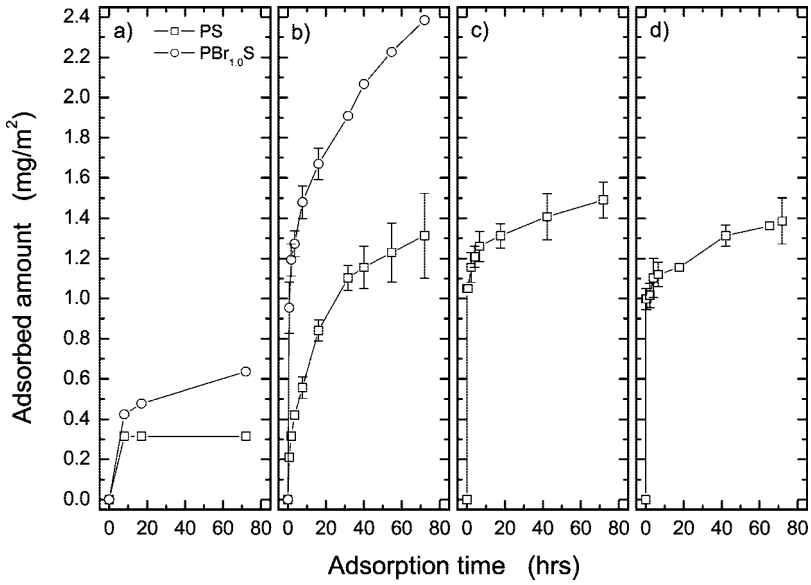

Figure 2. Adsorbed amount of polystyrene (□) and $PBr_{1.0}S$ (○) as a function of adsorption time for polymers adsorbing from (a) tetrahydrofuran at 25 °C, (b) toluene at 25 °C, (c) cyclohexane at 25 °C, and (d) cyclohexane at 50 °C. The polymer concentration in the solution was 1% (w/w). The lines are meant to guide the eye.

Table 1. Values of the Flory−Huggins Interaction Parameter for Various PS/Solvent and $PBr_{1.0}S$/Solvent Couples

system (temperature, °C)[a]	Flory−Huggins parameter, χ	Reference
PS/THF (25)	0.428[b]	76
PS/TOL (25)	0.432	77
PS/CH (25)	0.50	76
PS/CH (50)	0.48	76
$PBr_{1.0}S$/TOL(25)	0.64[c]	76

[a] PS: polystyrene, THF: tetrahydrofuran, TOL: toluene, CH: cyclohexane. [b] An alternative expression: $\chi_{PS/THF} = 0.474 - 0.073\phi_2$, where ϕ_2 is the volume fraction of polymer.[78] [c] This value is tabulated for the volume fraction of polymer, ϕ_2, of 0.4.

amount of $PBr_{1.0}S$ adsorbed on silica is about 4 times higher than that observed in the $PBr_{1.0}S$/THF system.

Having established the adsorption of homopolymers from various solvents, we now turn to discussing the adsorption of PBr_xS random RCPs onto SiO_x surfaces. Because of the small adsorbed amount of PS and $PBr_{1.0}S$ detected in THF-based system, we concentrated on RCP adsorption from TOL and CH. In Figure 3, we plot the amount of PBr_xS adsorbed onto silica from TOL solutions having 1% concentration of polymer (w/w). r-PBr_xS (■) and b-PBr_xS (●) copolymers with three different contents of 4-BrS were probed: (a) $x = 0.1$, (b) $x = 0.26 \pm 0.01$, and (c) $x = 0.60$ were used in these studies. To interpret the adsorption of the PBr_xS RCPs, we compare their behavior with homopolymer adsorption data for PS (□) and $PBr_{1.0}S$ (○). From the data in Figure 3a, it is evident that both r-$PBr_{0.1}S$ and b-$PBr_{0.1}S$ adsorb on silica surfaces in a manner similar to that of PS chains. Apparently, the concentration of 4-Br along PBr_xS is too small to cause any dramatic changes while adsorbing from TOL. In addition, no significant effect of comonomer distribution is detected in this system. Increasing the concentration of 4-BrS in PBr_xS from 10 to (26 ± 1)% causes detectable changes in the RCP adsorption (cf. Figure 3b). First, the adsorbed amount of r-$PBr_{0.25}S$ is higher than that of PS. Moreover, b-$PBr_{0.27}S$ adsorbs to the substrate more quickly than r-$PBr_{0.25}S$ (shorter diffusion times), but at long times, the monomer sequence distribution does not seem to influence the total adsorbed amount of RCP. The tendency of random-blocky copolymers to adsorb more strongly to the substrate, relative to the truly random RCPs, is also detected in the $PBr_{0.60}S$ system (cf. Figure 3c). Unlike in the $x = 0.26 \pm 0.01$ case, however, the total adsorbed amount

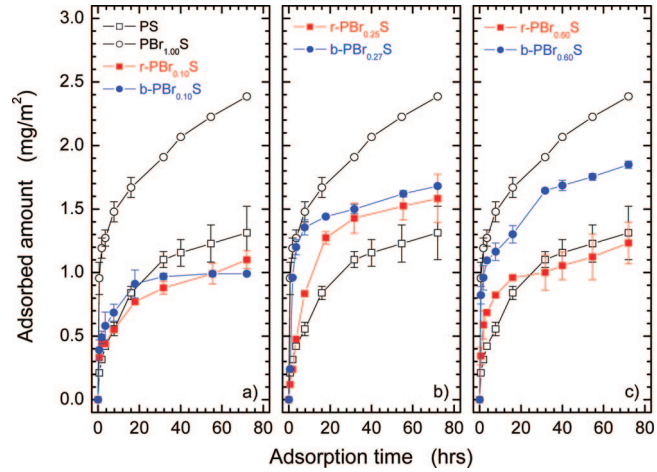

Figure 3. Adsorbed amount of polystyrene (□), $PBr_{1.00}S$ (○), r-PBr_xS (■), and b-PBr_xS (●) as a function of adsorption time for polymers adsorbing from toluene at 25 °C. The mole fraction of 4-BrS units in PBr_xS was (a) 0.10, (b) 0.26 ± 0.01, and (c) 0.60. The polymer concentration in the solution was 1% (w/w). The lines are meant to guide the eye.

of b-$PBr_{0.60}S$ exceeds that of r-$PBr_{0.60}S$ at long adsorption times. In fact, the data suggest that the amount of r-$PBr_{0.60}S$ adsorbed on the silica surface is comparable to that of PS. The data in Figure 4 reveal that essentially the same picture emerges when examining the adsorption of PBr_xS RCPs from TOL solutions having 2% concentration (w/w). There is no difference between r-$PBr_{0.1}S$ and b-$PBr_{0.1}S$ adsorbing onto silica; both polymers adsorb in amounts comparable to that of pure PS. Additionally, b-$PBr_{0.60}S$ adsorbs more strongly than r-$PBr_{0.60}S$; the adsorbed amount of the latter copolymer is comparable to that of PS.

In Figure 5, we plot the results of adsorption experiments conducted with PBr_xS solutions in CH. Specifically, the total adsorbed amount of r-PBr_xS (■) and b-PBr_xS (●) RCPs as a function of time is plotted for PBr_xS RCPs having $x = 0.10$ (parts a and b) and $x = 0.35$ (part c) adsorbing from solutions having a temperature of 25 °C (part a) and 50 °C (parts b and c). In all instances, we also provide corresponding adsorption data for PS homopolymer. Note that as mentioned previously, $PBr_{1.0}S$ was insoluble in CH at any temperature. Let us first

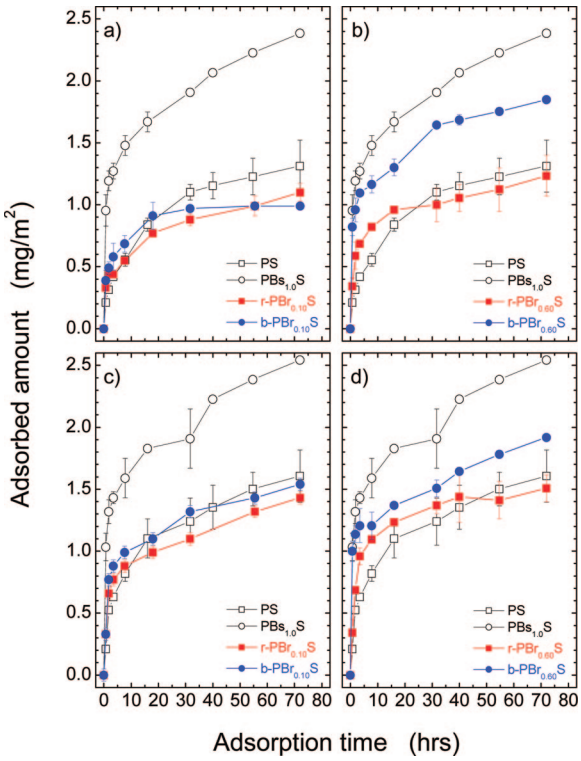

Figure 4. Adsorbed amount of polystyrene (□), PBr$_{1.0}$S (○), r-PBr$_x$S (■), and b-PBr$_x$S (●) as a function of adsorption time for polymers adsorbing from toluene at 25 °C. The mole fraction of 4-BrS units in PBr$_x$S was (a,c) 0.10 and (b,d) 0.60. The polymer concentration in the solution was (a,b) 1% (w/w) and (c,d) 2% (w/w). The lines are meant to guide the eye.

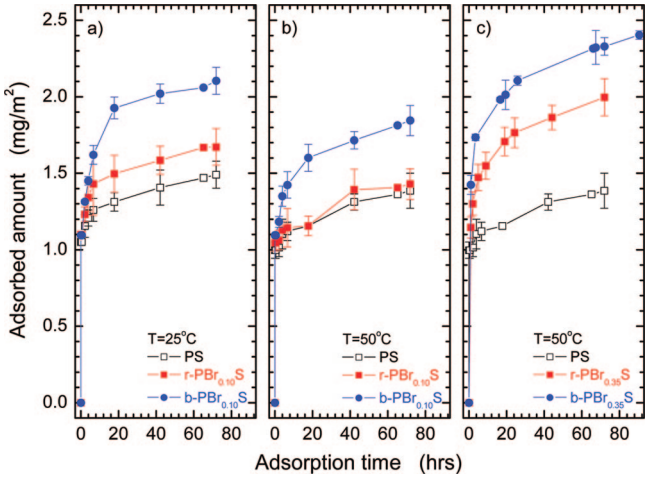

Figure 5. Adsorbed amount of polystyrene (□), r-PBr$_x$S (■), and b-PBr$_x$S (●) as a function of adsorption time for polymers adsorbing from cyclohexane at (a) 25 °C and (b,c) 50 °C. The mole fraction of 4-BrS units in PBr$_x$S was (a,b) 0.10 and (c) 0.35. The polymer concentration in the solution was 1% (w/w). The lines are meant to guide the eye.

concentrate on the adsorption results obtained from r-PBr$_{0.10}$S and b-PBr$_{0.10}$S. At 25 °C (cf. Figure 5a), the amount of b-PBr$_{0.10}$S adsorbed onto silica exceeds that of r-PBr$_{0.10}$S; the latter is higher than the amount of PS. At 50 °C the same trend is observed (cf. Figure 5b), namely, the adsorbed amount of b-PBr$_{0.10}$S is higher than that of r-PBr$_{0.10}$S; however, the overall magnitude of adsorption is lower than that observed at 25 °C. It is interesting to compare the adsorption of PBr$_{0.10}$S from TOL (cf. Figure 3a) with that from CH (cf. Figure 5a). In the latter case, a much stronger adsorption of both r-PBr$_{0.10}$S and

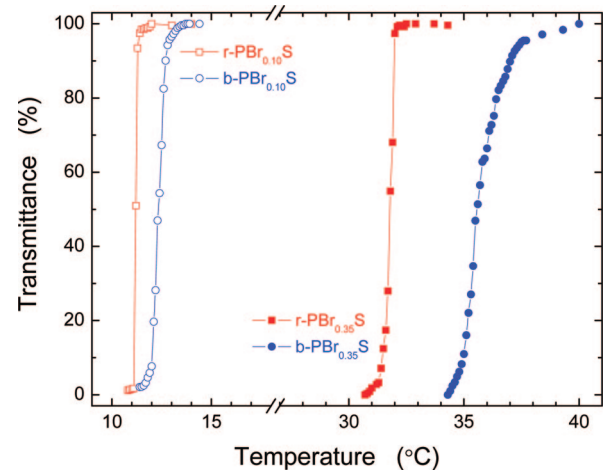

Figure 6. Transmittance through r-PBr$_x$S (squares) and b-PBr$_x$S (circles) with $x = 0.10$ (open symbols) and 0.35 (closed symbols) from cyclohexane solutions having a polymer concentration of 2% (w/w) ($x = 0.10$) and 1% (w/w) ($x = 0.35$) as a function of temperature. The lines are meant to guide the eye.

b-PBr$_{0.10}$S is detected, and a clear effect of the comonomer distribution is seen. We attribute this behavior to a much stronger repulsion between of 4-BrS and CH (relative to that between 4-BrS and TOL), $\chi_{4\text{-BrS/TOL}} \ll \chi_{4\text{-BrS/CH}}$. Assuming that the interaction energies of the solvent and polymer segments with silica do not change dramatically with temperature and that 4-BrS is equally insoluble in CH, the trend can be explained by considering the change in solvent quality for PS. Recall that the temperature is increased from 25 to 50 °C, CH changes from a good solvent to a θ solvent for PS. Figure 5c reveals that increasing the content of 4-BrS in PBr$_x$S from 10 to 35% leads to enhanced adsorption of PBr$_x$S. As previously observed for $x = 0.10$, the adsorbed amount of b-PBr$_{0.35}$S is higher than that of r-PBr$_{0.35}$S. There are two effects that likely contribute to the increased amount of PBr$_{0.35}$S at the silica interface relative to that of PBr$_{0.10}$S. First, the number of the adsorbing 4-BrS segments of PBr$_{0.35}$S having an attractive interaction with SiO$_x$ increases 3.5 times relative to that of PBr$_{0.10}$S. Second, at 50 °C, the solvent quality for PBr$_{0.35}$S is slightly worse relative to that of PBr$_{0.10}$S.[81] This is documented by cloud point measurements, shown in Figure 6. Specifically, the data in Figure 6 reveal two trends: (1) the solubility of PBr$_x$S decreases with increasing x, and (2) the solubility of b-Br$_x$S is lower than that of r-Br$_x$S for PBr$_x$S having the same content of 4-BrS. Overall, we attribute the enhanced amount of PBr$_x$S at the silica/solution interface associated with increasing the content of 4-BrS from 10 to 35% to the increase in the number of 4-BrS/SiO$_x$ contacts and temperature-dependent solubility of styrene segments in CH. We do not report on the adsorption of PBr$_{0.60}$S copolymers from CH solutions; our cloud point and small-angle neutron scattering measurements, to be reported in a separate publication,[84] reveal that PBr$_{0.60}$S/CH solutions are not homogeneous until heated to ~70 °C.

Theoretical Results. In this section, we present the main results from our computer simulation studies. These can be summarized as follows: (1) increasing the degree of "blockiness" enhances the adsorption of macromolecules dissolved in good solvents; (2) near the adsorption transition, the amount of adsorbed segments in random-blocky copolymers is larger relative to their regular multiblock counterparts; and (3) lowering the solvent quality facilitates copolymer adsorption. In general, these findings are in agreement with the experimental data previously discussed. We will now discuss the theoretical results in more detail.

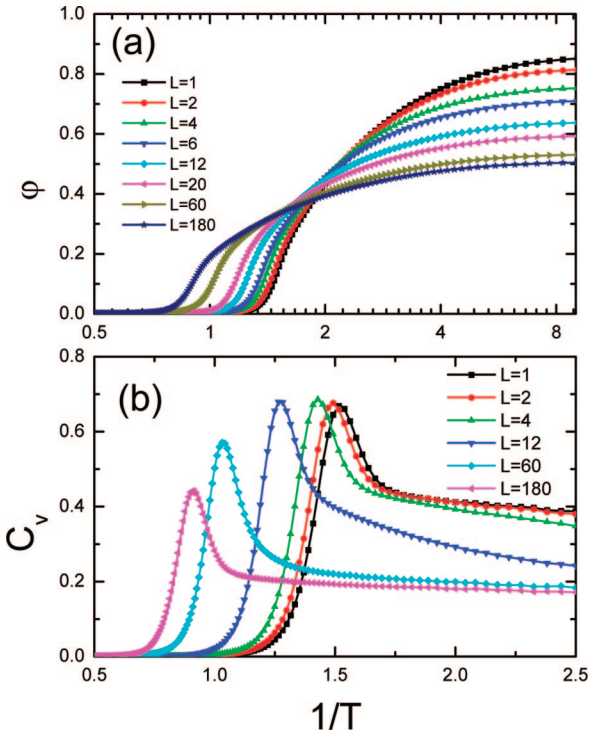

Figure 7. (a) Average fraction of adsorbed segments and (b) reduced heat capacity as a function of the reciprocal temperature for regular multiblock copolymers, $(A_LB_L)_m$, at different block lengths, L, and $\varepsilon_S = 0.5$.

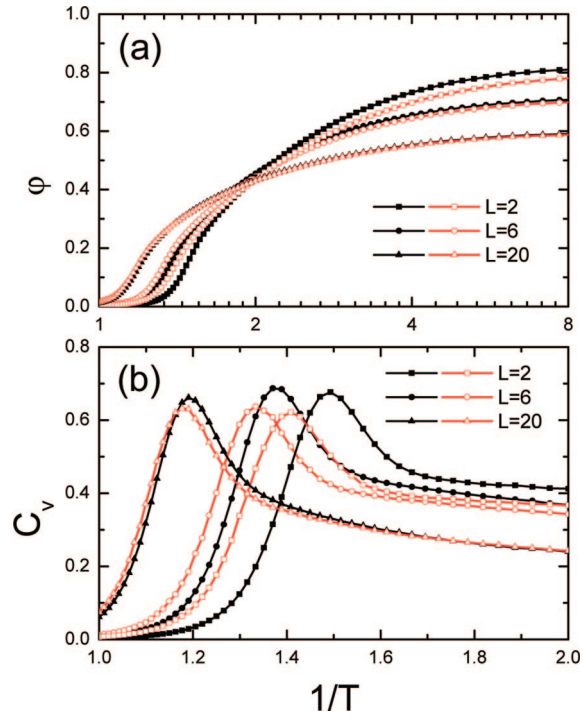

Figure 8. (a) Average fraction of adsorbed segments and (b) reduced heat capacity as a function of the reciprocal temperature for regular multiblock copolymers (closed symbols) and random-blocky copolymers (open symbols) at a few values of block length, L, and $\varepsilon_S = 0.5$. Each data point for random-blocky copolymers was obtained by averaging over 200 000 generated sequences.

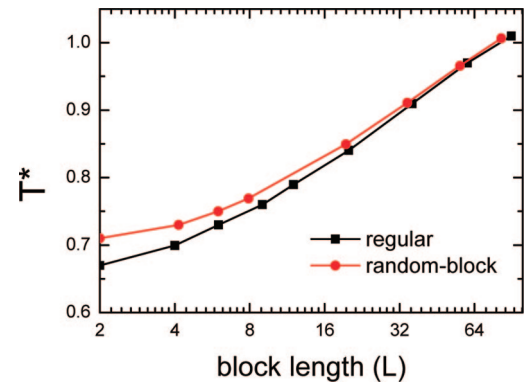

Figure 9. Critical adsorption temperature versus block length for regular and random-blocky copolymers.

In Figure 7a, we plot the average fraction of adsorbed polymer segments, φ, as a function of the inverse of the temperature, $1/T$, for the regular multiblock copolymers with different (fixed) block lengths L. The value of φ, which ranges from 0 to 1, can be considered to be an order parameter. At high temperatures, φ is small and increases with decreasing temperature. The curves rise over a narrow range of T; this increase becomes sharp for sufficiently low T, signaling an adsorption transition. Whereas these observations are expected, the most relevant for us is the fact that in the vicinity of the transition temperature, the amount of adsorbed polymer tends to increase with increasing block length, L; that is, the binding is promoted by a larger size of the adsorbing block. Therefore, the main feature of our results is the discovery of a preferential adsorption of copolymers with long adsorbing blocks. In general, this conclusion is in agreement with the experimental data discussed earlier and with a large body of various theoretical and simulation work cited in the Introduction. One might thus expect that for a block polymer system, polymers having the longest continuous run of the adsorbing segments should always be maximally adsorbed. In contrast, we find that at low enough temperature, the adsorption amount increases with decreasing length of the adsorbing block (cf. Figure 7a). Indeed, in the strong adsorption regime, all curves in Figure 7a tend to reach an asymptotic level, φ_{max}, which depends on L and decreases as L is increased. This finding can be understood from the fact that the long, weakly adsorbing B blocks tend to form entropically favored looplike sections surrounded by a good solvent. Therefore, the maximum loss in the conformational entropy is expected just for the long B blocks after they get strongly adsorbed to the surface.

The reduced heat capacity, $C_v = C_v/k_BN$, plotted in Figure 7b versus $1/T$, has a single sharp peak under a given solvent condition. The location of the maximum in heat capacity peaks defines the adsorption transition temperature, T^*. An increase in L is accompanied by the shift of the heat capacity peaks toward higher temperatures and by decrease in their intensity. We also detect that the peak becomes narrower as L increases. We therefore conclude that increasing the size of the adsorption block promotes the adsorption of periodic multiblock copolymers. That is, increasing the degree of "blockiness" enhances the adsorption of macromolecules dissolved in a good solvent, at least for the case in which the polymer−surface interaction is not very strong (cf. Figure 7a). The experimental data discussed above are in accord with this theoretical finding.

In Figures 8 and 9, we compare the properties of regular multiblock copolymers and random-blocky copolymers with a Poisson distribution of the block length. First, we find that near the adsorption transition, the amount of adsorbed segments in random-blocky copolymers, is larger relative to their regular counterparts at the same temperature and the same block length (cf. Figure 8a). In the case of sufficiently strong adsorption, however, we observe the opposite trend. For all of the temperature range investigated, the difference becomes less pronounced with increasing L; at $L = N/2$, the $\varphi(T)$ functions

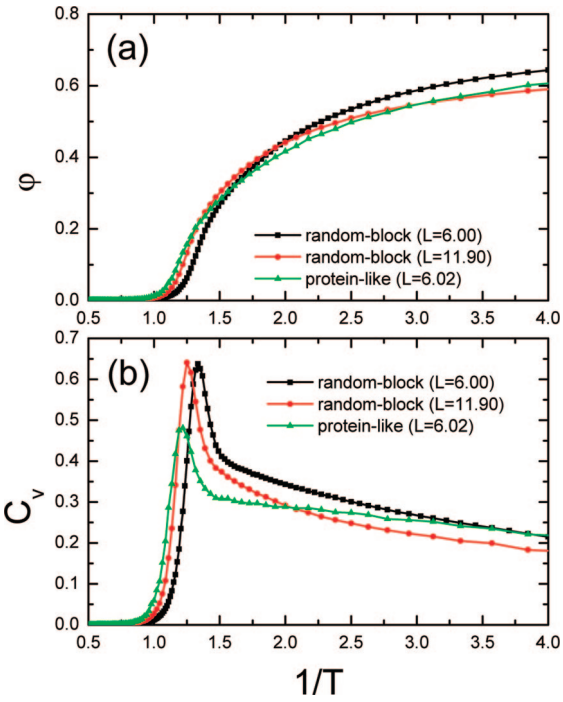

Figure 10. (a) Average fraction of adsorbed segments and (b) reduced heat capacity as a function of the reciprocal temperature for random-blocky copolymers and proteinlike copolymers at $\varepsilon_S = 0.5$. Each data point was obtained by averaging over 200 000 generated sequences.

coincide, as expected. Therefore, the adsorption behavior can be considerably modified by the polydispersity in block size distribution, particularly in the region near the transition temperature.

The data in Figure 8b reveal that at the same block size, the transition temperature, T^*, of the random-blocky copolymer is significantly higher relative to that of the regular block copolymer. Also, the introduction of block distribution polydispersity broadens the transition region to some extent. For a large L, however, the difference in the behavior of the two types of copolymers decreases. This is seen in Figure 9, which presents the dependence of T^* on L for both copolymers. We find the most pronounced difference between the T^* of the two copolymers for short blocks. When L approaches $N/2$ (i.e., the block size distribution $f(l)$ is strongly peaked around its maximum at $l = L$), the adsorption transition temperatures become indistinguishable for both systems. These results clearly demonstrate that the polydispersity in size distribution of chemically distinct blocks can have a marked effect on polymer adsorption. Note that the random-blocky copolymer with $L = 2$ corresponds to a "truly random" copolymer. Because it has the minimum T^* as compared with other random-blocky copolymers with larger L, we can conclude that the larger block lengths of adsorbing segments increase the probability of localizing such copolymers at the surface, which is in agreement with the experimental results.

To better understand how the polydispersity in block size distribution affects the adsorption of block copolymers, in Figure 10, we compare the properties of random-blocky and proteinlike (LF) macromolecules. At the same temperature and the same average block length, that is, $L = 6$, the fraction of adsorbed segments for the proteinlike macromolecules is noticeably higher than that for the random-blocky counterpart in the intermediate adsorption region (cf. Figure 10a). From the data presented in Figure 10b, we detect that the transition temperature for the 360-unit proteinlike copolymer with the average block length $L = 6.02$ is close to that of the random-blocky copolymer, in which the block length is roughly 2 times larger. These findings thus imply that the proteinlike copolymers are more "inclined" to adsorption than their random-blocky counterparts and regular multiblock chains.

The main conclusion that can be drawn from these results is as follows. There are two important factors that contribute to enhancing the selective copolymer adsorption: the block size and the block polydispersity. In particular, the presence of block polydispersity tends to raise the critical adsorption temperature sharply relative to the monodisperse limit. Therefore, upon increasing the degree of block distribution polydispersity at a given temperature, one can expect the adsorption to become stronger. Our results provide extreme examples of such a behavior. For instance, at $L = 6$, the temperature, at which we observe adsorption transition in the polydisperse systems ($T^* = 0.75$ and 0.82 for the present random-blocky and proteinlike model copolymers, respectively) exceeds the corresponding critical temperature in the monodisperse limit, namely, $T^* = 0.73$ (cf. Figures 9 and 10b). Therefore, at $T \geq 0.75$, no adsorption transition would occur at all in the monodisperse limit for this chain length and block size. Obviously, these features demonstrate that the block distribution polydispersity has a profound effect on adsorption.

The key reason behind this distinction is that the behavior of RCPs is governed by not only the average block length, L, but also the variance of the block length, D. For RCPs, many properties are dominated by long blocks whose probability of occurrence increases with increasing D. Even at a relatively low fraction of these blocks in the chain, their effect can be decisive. As we stressed while discussing Figure 9, the largest differences between the regular and random-blocky copolymers manifest themselves just at relatively small L values when the chain consists of both the short and rather long chemically homogeneous sections. Increasing L at fixed N leads to a decrease in the width of the block length distribution, $f(l)$; the differences gradually disappear (cf. Figure 9). As briefly mentioned previously, the block length distribution in proteinlike copolymers is described by a specific type of statistics, namely, by the statistics of Lévy-flight type.[68] This distribution is characterized by a very high D for long chains. That is why the proteinlike chains contain a significant fraction of long sections composed of chemically identical segments, even at relatively small L values. This is the major reason behind the rather unusual adsorption behavior of such copolymers.

It has long been appreciated that the compositional polydispersity can profoundly influence the properties of polymers. To this end, the majority of recent efforts has focused on clarifying the bulk phase behavior of polydisperse polymer systems (see, e.g., refs 54 and 85 for recent reviews). In the case of adsorption, the block polydispersity manifests itself as a fractionation effect: a mixture of different "copolymer species" described by some "parent" distribution $f(l)$ separates into several fractions, each of which differs in monomer sequence distribution from the parent sequence; the maximally adsorbed fraction contains chains with the longest adsorption blocks. Owing to the effect of fractionation, the adsorbed phase is enriched in large-block polymer species.

After this work was written, a paper by Bhattacharya et al.[86] appeared in which the authors simulated single-chain adsorption of regular multiblock AB copolymers and truly random AB copolymers with excluded volume interaction. It is important to stress that their results obtained for regular multiblock copolymers are generally very close to those described in this study. In particular, they predicted that the critical adsorption temperature is an increasing function of block length, L.

Having examined the role of block size and polydispersity, we now turn to consider the variation of adsorption properties

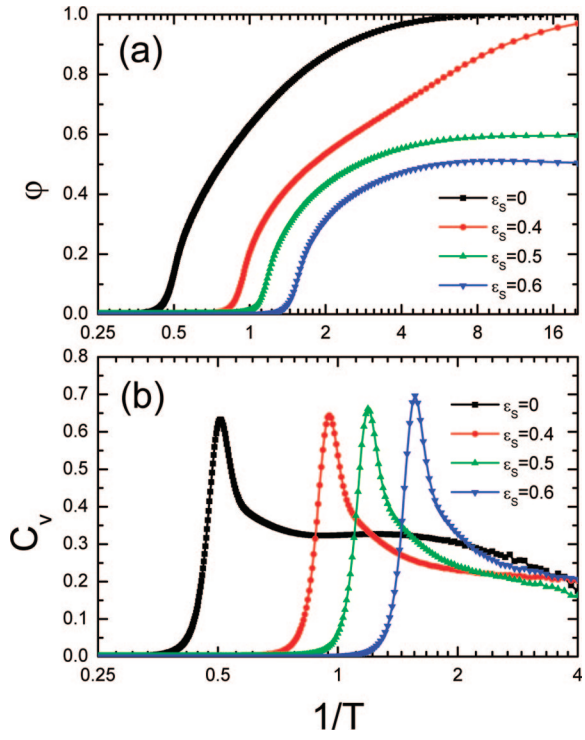

Figure 11. (a) Average fraction of adsorbed segments and (b) reduced heat capacity as a function of the reciprocal temperature for regular multiblock copolymer, $(A_{20}B_{20})_9$, at different monomer−solvent strengths, ε_S.

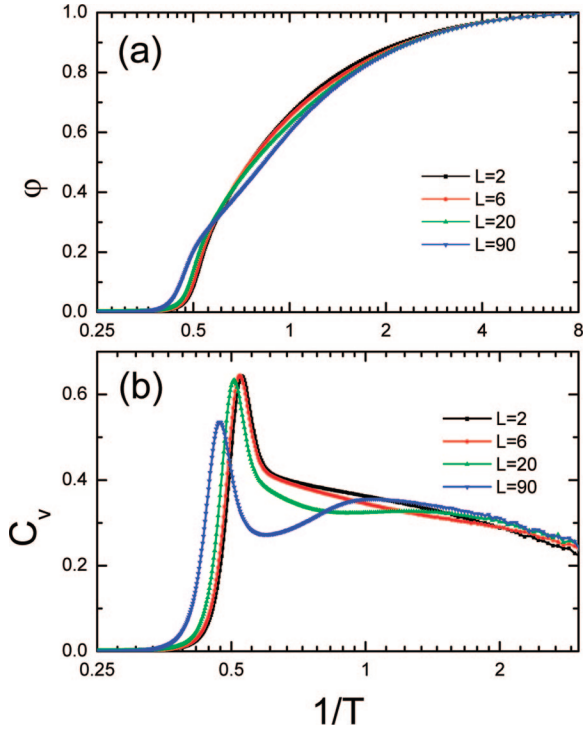

Figure 12. (a) Average fraction of adsorbed segments and (b) reduced heat capacity as a function of the reciprocal temperature for regular multiblock copolymers, $(A_LB_L)_m$, at different block lengths, L, and $\varepsilon_S = 0$.

under different solvent conditions. The data in Figures 11 and 12 illustrate the effect of polymer−solvent interactions on φ and C_v for block copolymers with fixed L. Note that upon decreasing ε_S, the solvent quality becomes worse; the case $\varepsilon_S = 0$ corresponds to an athermal solvent. As expected, lowering the solvent quality facilitates adsorption (cf. Figure 11a). Similar

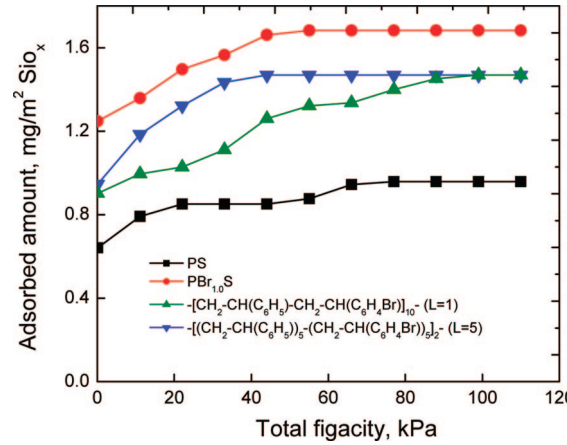

Figure 13. Adsorption isotherms calculated for 20-unit copolymer chains $PBr_{0.5}S$ having different degree of blockiness ($L = 1$ and 5) and for PS and $PBr_{1.0}S$ homopolymers at $T = 298$ K. The lines are meant to guide the eye.

trends associated with varying the solvent quality are observed for the brominated PSs dissolved in CH or TOL (cf. Figures 2−5).

In the strong adsorption limit and at small ε_S ($\varepsilon_S \ll \varepsilon_B$), it is expected that $\varphi \to 1$ for any L. In contrast, in the case of large ε_S ($\varepsilon_S > \varepsilon_B$) and low T, one has $\varphi = {}^1/_2$ for the selectively adsorbing symmetric block copolymers under study. These trends are seen in Figures 8 and 10.

From the data shown in Figure 11b, we conclude that upon decreasing solvent quality, the transition temperature, defined by the position of the heat capacity peak, increases. That behavior is in qualitative agreement with the experimental observation discussed above (cf. Figure 6). In the case of an athermal solvent, it is possible to identify two peaks in the heat capacity (cf. Figures 11b and 12b), which correspond to adsorption transitions of the chemically different blocks. The peak at lower temperatures is weaker and diffused relative to the other one. Therefore, for not very good solvents, we observe a two-step process of copolymer adsorption. At the first step, the AB copolymer adsorbs onto the surface as an effective homopolymer. After the first adsorption transition, more A monomers with higher interaction energy get adsorbed on the surface, whereas more of weakly adsorbing B monomers remain nonadsorbed. At lower temperatures, local rearrangements of the partially adsorbed polymer chain take place, a process that is accompanied by the adsorption of B blocks and by the appearance of the second weak peak in the heat capacity. These results are in agreement with the recent Monte Carlo simulation of Sumithra and Straube.[87]

Finally, let us briefly discuss the results from our atomistic simulations. We have calculated the average loading of the $PBr_{0.5}S$ copolymers and the PS and $PBr_{1.0}S$ homopolymers on a flat silica surface over a wide range of pressures. The pressure (fugacity) was varied from $P = 0.1$ to 120 kPa while the temperature was fixed at $T = 298$ K. The loading at each point in the pressure range was calculated, and the points were combined to obtain adsorption isotherms. The adsorption isotherm characterizes the affinity of the sorbate component toward the adsorbing surface and can, in principle, be directly compared with experimental measurements. In Figure 13, we plot the adsorption isotherms calculated for the $PBr_{0.5}S$ copolymers having different degree of blockiness, L. The results are compared with those obtained for the PS and $PBr_{1.0}S$ homopolymers of the same length. First, we find that $PBr_{1.0}S$ adsorbs much more strongly than PS. Second, the partially brominated PSs possess higher affinity for the silica surface than PS but worse

affinity than that observed for $PBr_{1.0}S$. Finally, it is seen that the copolymer chains having a more blocky character ($L = 5$) exhibit a stronger adsorption relative to their short-block (alternating) counterparts ($L = 1$). The difference in the adsorbed amount of the short-block and long-block copolymers decreases as the pressure is increased. From the simulation, we conclude that the interplay between the partitioning of long and short blocks of consecutive adsorbing monomers within the chain is responsible for the observed difference in the copolymer adsorption. In principle, the same conclusion follows from the experimental measurements. Moreover, the simulation predicts the adsorbed amounts of the polymers almost in quantitative agreement with the experimental data.

Summary

This article presented a combined experimental and computer simulation study aimed at understanding the adsorption of RCPs at flat impenetrable substrates. In the experimental part, we presented and discussed the adsorption of RCP poly(styrene-co-4-bromostyrene) (PBr_xS), where x denotes the mole fraction of 4-BrS onto flat silica surfaces. Our results demonstrated that the adsorption of PBr_xS increased with: (1) increasing blockiness of the macromolecule, (2) increasing content of 4-BrS in PBr_xS, and (3) decreasing solvent quality. These results represent the first systematic experimental study revealing the effect of the comonomer distribution in RCPs on flat impenetrable surfaces.

The theoretical part of the article aimed at providing molecular-level insight into our experimental findings. To simulate copolymer adsorption, we used two models: (1) a coarse-grained statistical mechanical model based on the approach recently developed by Kriksin et al.[67] and (2) a fully atomistic model combined with the CB-GCMC simulation technique. The selective adsorption of both regular and random multiblock copolymers was investigated in detail. From the computer simulations, we concluded that increasing the degree of copolymer "blockiness" enhanced the adsorption of macromolecules dissolved in a good solvent, at least for the case in which the polymer−surface interaction was not very strong. The same behavior was observed in our experiments. The calculations predicted that the larger block lengths of adsorbing segments increased the probability of localizing the RCPs at the surface, which is in agreement with the experimental results. It was also demonstrated that the polydispersity in size distribution of chemically distinct blocks had a profound effect on polymer adsorption. Two important ingredients contributed to enhancing the selective copolymer adsorption: the block size and the block distribution polydispersity. In particular, the presence of block polydispersity tended to raise the critical adsorption temperature sharply relative to the monodisperse limit. The effect of solvent quality was also simulated. As expected, lowering the solvent quality facilitated adsorption. Similar trends associated with varying the solvent quality were observed for the brominated PSs dissolved in CH or TOL. For not very good solvents, we observed a two-step process of copolymer adsorption accompanied by the presence of two distinct maxima on the heat capacity curve: one that was associated with a weak polymer-surface complexation, when the copolymer "stuck" to the surface as an effective homopolymer, and the other that occurred at stronger adsorption, when more chain segments with higher interaction energy got adsorbed, whereas more of the weakly adsorbing segments remained nonadsorbed.

Acknowledgment. This work at NC State University was supported by the National Science Foundation under contract nos. DMR-0353102 and OISE-0730243. P.G.K. and A.R.K. gratefully acknowledge financial support from RFBR and from Deutsche Forschungsgemainschaft within the SFB 569 program (projects B13 and A11).

References and Notes

(1) Lee, L. H. *Adhesion and Adsorption of Polymer*; Plenum Press: New York, 1980.
(2) Napper, D. H. *Polymeric Stabilization of Colloidal Dispersions*; Academic Press: London, 1983.
(3) Tseng, C. M.; Lu, Y. Y.; El-Aasser, M. S.; Vanderhoff, J. W. *J. Polym. Sci., Polym. Chem. Ed.* **1986**, *24*, 2995.
(4) Ober, C. K.; Hair, M. L. *J. Polym. Sci., Polym. Chem. Ed.* **1987**, *25*, 1395.
(5) Ruckenstein, E.; Chang, D. B. *J. Colloid Interface Sci.* **1988**, *123*, 170.
(6) Tadros, Th. F. *Polym. J.* **1991**, *23*, 5.
(7) *Coagulation and Flocculation: Theory & Applications*; Dobiás, B., Ed.; Marcel Dekker: New York, 1993.
(8) Jenkel, E.; Rumbach, B. *Z. Elektrochem.* **1951**, *55*, 612.
(9) Silberberg, A. *J. Phys. Chem.* **1962**, *66*, 1872.
(10) DiMarzio, E. A. *J. Phys. Chem.* **1965**, *42*, 2101.
(11) Chan, D. *J. Chem. Soc., Faraday Trans.* **1975**, *71*, 235.
(12) Lax, M. *Macromolecules* **1974**, *7*, 660.
(13) Feigin, R. I.; Napper, D. H. *J. Colloid Interface Sci.* **1979**, *71*, 117.
(14) Takahashi, A.; Kawaguchi, M. *Adv. Polym. Sci.* **1982**, *46*, 1.
(15) Fleer, G. J.; Cohen Sturat, M. A.; Cosgrove, T.; Scheutjens, J. M. H. M.; Vincent, V. *Polymers at Interfaces*; Chapman & Hall: London, 1993.
(16) Birstein, T. M.; Borisov, O. V. *Polymer* **1991**, *32*, 923.
(17) Klushin, L. I.; Skvortsov, A. M.; Gorbunov, A. A. *Phys. Usp.* **1998**, *41*, 639–649.
(18) Balazs, A. C.; Gempe, M.; Lantman, C. W. *Macromolecules* **1991**, *24*, 168.
(19) Motchmann, H.; Stamm, M.; Toprakcioglu, Ch. *Macromolecules* **1991**, *24*, 3681.
(20) Yeung, C.; Balazs, A. C.; Jasnow, D. *Macromolecules* **1992**, *25*, 1357.
(21) Guzonas, D. A.; Bois, D.; Tripp, C. P.; Hair, M. L. *Macromolecules* **1992**, *25*, 2434.
(22) Leclerc, E.; Daoud, M.; Douillard, R. *Nuovo Cimento Soc. Ital. Fis., D* **1994**, *16*, 641.
(23) Gutman, L.; Chakraborty, A. K. *J. Chem. Phys.* **1996**, *104*, 7306.
(24) Gutman, L.; Chakraborty, A. K. *J. Chem. Phys.* **1996**, *105*, 7842.
(25) Bratko, D.; Chakraborty, A. K.; Shakhnovich, E. I. *Chem. Phys. Lett.* **1997**, *280*, 46.
(26) Chakraborty, A. K.; Bratko, D. *J. Chem. Phys.* **1998**, *108*, 1676.
(27) Simmons, E. R.; Chakraborty, A. K. *J. Chem. Phys.* **1998**, *109*, 8667.
(28) Bratko, D.; Chakraborty, A. K.; Shakhnovich, E. I. *Comput. Theor. Polym. Sci.* **1998**, *8*, 113.
(29) Zheligovskaya, E. A.; Khalatur, P. G.; Khokhlov, A. R. *Phys. Rev. E* **1999**, *59*, 3071.
(30) Genzer, J. *Adv. Colloid Interface Sci.* **2001**, *94*, 105.
(31) Genzer, J. *Macromol. Theory Simul.* **2002**, *11*, 481.
(32) Whittington, S. G. *Physica A* **2002**, *314*, 214.
(33) Dadmun, M. *Macromolecules* **1996**, *29*, 3868.
(34) Benkoski, J. J.; Fredrickson, G. H.; Kramer, E. J. *J. Polym. Sci., Part B: Polym. Phys.* **2001**, *39*, 2363.
(35) Bucknall, D. G. *Prog. Mater. Sci.* **2004**, *49*, 713.
(36) Chuang, J.; Grosberg, A.; Kardar, M. *Phys. Rev. Lett.* **2001**, *87*, 078104.
(37) Yamagiwa, S.; Kawaguchi, M.; Kato, T.; Takahashi, A. *Macromolecules* **1989**, *22*, 2199.
(38) Kawaguchi, M.; Itoh, K.; Yamagiwa, S.; Takahashi, A. *Macromolecules* **1989**, *22*, 2204.
(39) Ermoshkin, A. V.; Chen, J. Z. Y.; Lai, P. Y. *Phys. Rev. E* **2002**, *66*, 051912.
(40) Moghaddam, A. S.; Whittington, S. G. *J. Phys. A: Math Gen.* **2002**, *35*, 33.
(41) Moghaddam, A. S. *J. Phys. A: Math Gen.* **2003**, *36*, 939.
(42) Cosgrove, T.; Finch, N. A.; Webster, J. R. P. *Macromolecules* **1990**, *23*, 3353.
(43) Balazs, A. C.; Gempe, M. *Macromolecules* **1991**, *24*, 168.
(44) Sumithra, K.; Baumgaertner, A. *J. Chem. Phys.* **1998**, *109*, 1540.
(45) Sumithra, K.; Baumgaertner, A. *J. Chem. Phys.* **1999**, *110*, 2727.
(46) Orlandini, E.; Tesi, M. C.; Whittington, S. G. *J. Phys. A: Math. Gen.* **1999**, *32*, 469.
(47) Liu, H.; Chakrabarti, A. *Polymer* **1999**, *40*, 7185.
(48) Khokhlov, A. R.; Khalatur, P. G. *Physica A* **1998**, *249*, 253.
(49) Khalatur, P. G.; Ivanov, V. I.; Shusharina, N. P.; Khokhlov, A. R. *Russ. Chem. Bull.* **1998**, *47*, 855.
(50) Khokhlov, A. R.; Khalatur, P. G. *Phys. Rev. Lett.* **1999**, *82*, 3456.
(51) van den Oever, J. M. P.; Leermakers, F. A. M.; Fleer, G. J.; Ivanov, V. A.; Shusharina, N. P.; Khokhlov, A. R.; Khalatur, P. G. *Phys. Rev. E* **2002**, *65*, 041708.

(52) Khalatur, P. G.; Novikov, V. V.; Khokhlov, A. R. *Phys. Rev. E* **2003**, *67*051901.
(53) Khokhlov, A. R.; Khalatur, P. G. *Curr. Opin. Solid State Mater. Sci.* **2004**, *8*, 3.
(54) For a recent review see: Khalatur, P. G.; Khokhlov, A. R. *Adv. Polym. Sci.* **2006**, *195*, 1, and references therein.
(55) (a) Lozinsky, V. I.; Simenel, I. A.; Kurskaya, E. A.; Kulakova, V. K.; Grinberg, V. Ya.; Dubovik, A. S.; Galaev, I. Yu.; Mattiasson, B.; Khokhlov, A. R. *Rep. Russ. Acad. Sci.* **2000**, *375*, 637. (b) Wahlund, P.-O.; Galaev, I. Yu.; Kazakov, S. A.; Lozinsky, V. I.; Mattiasson, B. *Macromol. Biosci.* **2002**, *2*, 33.
(56) Lozinsky, V. I. *Adv. Polym. Sci.* **2006**, *196*, 87, and references therein.
(57) Siu, M.-H.; Zhang, G.; Wu, C. *Macromolecules* **2002**, *35*, 2723.
(58) Semler, J. J.; Jhon, Y. K.; Tonelli, A.; Beevers, M.; Krishnamoorti, R.; Genzer, J. *Adv. Mater.* **2007**, *19*, 2877.
(59) Jhon, Y. K.; Semler, J.; Genzer, J. *Macromolecules* **2008**, *41*, 6719.
(60) Tonelli, A. E. *Macromolecules* **1977**, *10*, 153.
(61) Khanarian, G.; Cais, R. E.; Kometani, J. M.; Tonelli, A. E. *Macromolecules* **1982**, *15*, 866.
(62) Jhon, Y. K.; Krishanmoorti, R.; Genzer, J. Unpublished data.
(63) Semler, J. J.; Jhon, Y. K.; Beevers, M.; Tonelli, A.; Genzer, J. Unpublished results.
(64) *Handbook of Ellipsometry*; Tompkins, H. G., Irene, E. A., Eds.; William Andrew Publishing: Norwich, NY, 2005.
(65) The index of refraction of PBr1.0S was measured on a spin-coated PBr1.0S film on a silicon wafer by a variable angle spectroscopic ellipsometer (J.A. Woollam Co., Inc.).
(66) Strobl, G. R.; Urban, G. *Colloid Polym. Sci.* **1998**, *266*, 398.
(67) Kriksin, Yu. A.; Khalatur, P. G.; Khokhlov, A. R. *J. Chem. Phys.* **2005**, *122*, 114703; **2006**, *124*, 174904.
(68) Govorun, E. N.; Ivanov, V. A.; Khokhlov, A. R.; Khalatur, P. G.; Borovinsky, A. L.; Grosberg, A. Y. *Phys. Rev. E* **2001**, *64*, 040903.
(69) *Lévy Flights and Related Topics in Physics*; Shlesinger, M. F., Zaslavsky, G. M., Frisch, U., Eds.; Springer-Verlag: Berlin, 1996.
(70) Siepmann, J. I.; Frenkel, D. *Mol. Phys.* **1992**, *75*, 59.
(71) Smit, B. *Mol. Phys.* **1995**, *85*, 153.
(72) Frenkel, D.; Mooij, G.; Smit, B. *J. Phys.: Condens. Matter* **1992**, *4*3053.
(73) (a) Garofalini, S. H. *J. Non-Cryst. Solids* **1990**, *120*, 1. (b) Litton, D. A.; Garofalini, S. H. *J. Appl. Phys.* **2001**, *89*, 6013.
(74) Hwang, M. J.; Stockfisch, T. P.; Hagler, A. T. *J. Am. Chem. Soc.* **1994**, *116*, 2515.
(75) Maple, J. R.; Hwang, M.-J.; Stockfish, T. P.; Dinur, U.; Waldman, M.; Ewig, C. S.; Hagler, A. T. *J. Comput. Chem.* **1994**, *15*, 162–182.
(76) *Polymer Handbook*; Brandrup, J., Immergut, E. H., Grulke, E. A., Abe, A., Bloch, D. R., Eds.; Wiley-Interscience: New York, 2005.
(77) Van der Beek, G. P.; Cohen, Stuart, M. A.; Fleer, G. J.; Hofman, J. E. *Macromolecules* **1991**, *24*, 6600.
(78) Shiomi, T.; Kuroki, K.; Kobayashi, A.; Nikaido, H.; Yokoyama, M.; Tezuka, Y.; Imai, K. *Polymer* **1995**, *36*, 2443.
(79) Brei, V. V.; Gorlov, Y. I.; Konoplya, M. M.; Nazarenko, V. A.; Chuiko, A. A. *Theor. Exper. Chem.* **1984**, *19*, 671.
(80) Ringwald, S.; Pemberton, J. E. *Environ. Sci. Technol.* **2000**, *34*, 259.
(81) Bródka, A. *Mol. Phys.* **1994**, *83*, 803.
(82) Tsitsilianis, C.; Pierri, E.; Dondos, A. *J. Polym. Sci., Polym. Ed.* **1983**, *21*, 685.
(83) Oslanec, R.; Composto, R. J.; Vlcek, P. *Macromolecules* **2000**, *33*, 2200.
(84) The cloud points for $PBr_{0.10}S$ are ∼13 °C (random) and ∼12.5 °C (random-blocky) and those of $PBr_{0.35}S$ are ∼32 °C (truly random) and ∼36 °C (random-blocky). Note that the cloud point temperature for b-PBr_xS is consistently higher than that of r-PBr_xS; the difference between the two cloud point temperatures increases upon increasing the degree of bromination (x) [Jhon, Y. K.; Krishanmoorti, R.; Genzer, J. In preparation.].
(85) Fredrickson, G. H. *The Equilibrium Theory of Inhomogeneous Polymers*; International Series of Monographs on Physics 134; Oxford University Press: New York, 2006.
(86) Bhattacharya, S.; Hsu, H.-P.; Milchev, A.; Rostiashvili, V. G.; Vilgis, T. A. *Macromolecules* **2008**, *41*, 2920–2930.
(87) Sumithra, K.; Straube, E. *J. Chem. Phys.* **2006**, *125*, 154701.

MA8027936